Chin. J. Chem. Eng., **15**(4) 545—553 (2007)

Modeling and Simulation of Heterogeneous Catalyzed Propylene Polymerization*

LIU Xinggao(刘兴高)**
State Key Laboratory of Industrial Control Technology, Institute of Industrial Control, Department of Control Science and Technology, Zhejiang University, Hangzhou 310027, China

Abstract A novel mathematical model for single particle slurry propylene polymerization using heterogeneous Ziegler-Natta catalysts has been developed to describe the kinetic behavior, the molecular weight distribution, the monomer concentration, the degree of polymerization, the polydispersity index (PDI), *etc*. This model provides a more valid mathematical description by accounting for the monomer diffusion phenomena at two levels as multigrain model counts, and obtains results that are more applicable to the conditions existing in most polymerizations of industrial interest. Considering that some models on the mesoscale phenomena are so complex that some existing modeling aspects have to be simplified or even neglected to make the model convenient for use in interesting engineering studies, it is very important to put some effort into determining what sort of numerical analysis works best for these problems. For this reason, special attention is paid to these studies to explore an efficient algorithm using adaptive grid-point spacing in a finite-difference technique to figure out more practical mass transport models and convection-diffusion models efficiently. The reasonable outcomes, as well as the significant computation time saving, have been achieved, thereby displaying the advantage of this calculation method.
Keywords modeling and simulation, propylene polymerization, mass transfer, diffusion and convection

1 INTRODUCTION

Production of polyolefins is a multi-billion dollar business[1]. Owing to the relatively high complexity and multiscale nature[2] with respect to not only space but also time of the kinetic behavior and operation in polyolefin plants, decision making may rely on simulations performed with complex mathematical models of the polymerization process. For this reason, a significant number of articles have been published regarding the modeling and simulation of olefin polymerization reactors in the last two decades. One can associate different characteristic lengths and phenomena with three different levels: macroscale, mesoscale, and microscale, respectively[3—5]. This article concentrates on the mesoscale phenomena. For more information on mesoscale models, the purely diffusional resistances with supported heterogeneous Ziegler-Natta catalyzed propylene polymerization have been modeled in the form of the solid core model (SCM)[6,7], the polymeric flow model (PFM)[7,8], and later more elaborately in the form of the multigrain model (MGM)[6,9,10] and the polymeric multigrain model (PMGM)[11,12].

The MGM model of Floyd *et al*.[9] shown schematically in Fig.1 considers the transport phenomena within the particle at two distinct levels, where both

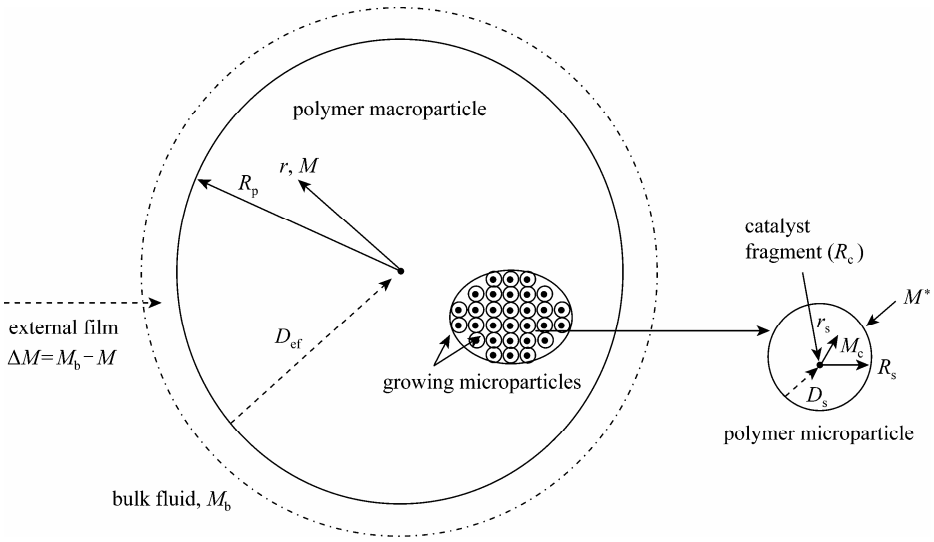

Figure 1 Schematic diagram of particle growth in MGM and PMGM models

Received 2006-05-11, accepted 2007-02-01.
* Supported by the National High Technology Development Program of China (No.2006AA05Z226), Natural Science Foundation of Zhejiang Province (No.Y105370), National HI-TECH Industrialization Program of China (No.2004-2080), and Science Fund for Distinguished Young Scholars of Zhejiang University (No.111000-581645).
** To whom correspondence should be addressed. E-mail: liuxg@iipc.zju.edu.cn

large scale diffusion through the macroparticle (D_{ef}) and microparticle diffusion (D_s) through the polymer film surrounding the catalyst fragments are considered. MGM is probably the most comprehensive one of the pure Fichian diffusional models, particularly since it can incorporate catalyst fragmentation, diffusional resistance, as well as active site heterogeneity, which are the three most important physicochemical effects. The major disadvantage of this model is that the computational times required to obtain the Polydispersity index (PDIs) are extremely high. This disadvantage makes this model inconvenient for use in interesting engineering studies like the simulation of industrial reactors, optimization, control, *etc*.

For this reason, studies on the PMGM model by Sarkar and Gupta[11,12] lead to the development of more diffusion that is negligible as shown in Fig.1, where microparticle diffusion, D_s, at the microparticle level is negligible, and a formulation similar to that of Laurence and Chiovetta[13] is adopted with specified size and porosity data. The main advantage of this model is that its solution method makes the computational rate improve significantly by employing clubbed shell computational algorithm (CSA)[12]. Unfortunately, some results from PMGM are not very applicable to the conditions existing in most polymerization of industrial interest, such as the monomer concentration at the centre of the particles drops very quickly to nearly zero, and remains there for over 2h of polymerization[3]; as well as PMGM assumes that the change of the number of microparticles does not lead to considerable change in the result, which differs from the Nagel's research[6] while varying the initial radius of catalyst microparticle (R_c) with the initial particle radius of catalyst macroparticles (R_0) constant.

All models on the mesoscale phenomena presented above are pure Fickian diffusion models, most results of which agree reasonably well with the experimental measurement for both microparticles and macroparticles. However, as these fail to explain the intrinsic activity now attainable, the requirement for incorporating monomer convection, which is thought to be driven by the pressure gradient created by the monomer consumption within the particle, in such a model is essential[14].

The main purpose of this study, therefore, is to introduce a modified model extended from the polymeric multigrain model with an improved algorithm to model industrial problems, where additional physicochemical effects and assumptions can be added as well as there is a high solving efficiency. The relevant outcomes, figured out from this modified model in the area of intraparticle mass transfer for slurry propylene polymerization with Ziegler-Natta catalyst, are more suitable for industrial application when compared with the original PMGM model of Sarkar and Gupta[11]. Additionally, this kind of algorithm, extended from PMGM[12] as an alternative method for solving the monomer conservation equations to accelerate the computational time significantly besides maintaining the results reasonably, is further applied to the convection-diffusion model, which considers the monomer convection through interconnected pores in the macroparticle to explain some phenomenon that pure Fickian's diffusion model fails to reach under certain circumstance.

2 THEORY

2.1 Modified polymeric multigrain model

The slurry propylene polymerization is considered to contrast with PMGM. The radii of the microparticle (R_c) are all assumed to be of the same value according to Kakugo's experiment, which advances that all radii of the catalyst subparticle remain the same and unchanged after experiencing the instantaneous fragmentation during the process of polymerization[15]. The consideration is limited to homopolymerization, spherical catalyst particle, a single type of active site, isothermal, and negligible heat transfer[16,9,10], and the assumption of instantaneous rupture is retained, which is also employed by SCM, PFM, MGM and PMGM[16,17]. The case in which there is termination by transfer to hydrogen owing to its predominance is considered. Since the main objective of this article is to demonstrate the efficiency of the modified polymeric multigrain model with clubbing, the simplified mechanism of Ziegler-Natta catalyzed propylene polymerization is adopted, as shown in Table 1.

Table 1 Simplified kinetic mechanism of Ziegler-Natta catalyzed propylene polymerization

	Reaction
initiation	$P_0 + M_c \xrightarrow{k_p} P_1$
propagation	$P_n + M_c \xrightarrow{k_p} P_{n+1}$
termination	$P_n + \frac{1}{2}H_2 \xrightarrow{k_{tr}} D_n + P_1$

where, P_0 represents the unreacted active catalyst sites, while P_n, which is still attached to an active site, and D_n, which has at its end, a group from a chain transfer or deactivating agent, are the concentrations of the live and dead polymer of chain length n, respectively. Both rate constants for initiation and propagation are represented by k_p. k_{tr} represents the termination by chain transfer to hydrogen.

The following well-known diffusion-reaction differential equations are obtained for the concentration of the monomer at any radial position, r, and time, t, in the growing porous spherical polymer particle for the fluid diffusion phenomena at two different scales:

$$\frac{\partial M}{\partial t} = \frac{D}{r^2}\frac{\partial}{\partial r}\left(r^2 \frac{\partial M}{\partial r}\right) - R_{pv} \tag{1a}$$

$$\frac{\partial M}{\partial r}(r=0,t) = 0 \tag{1b}$$

$$D_{ef}\frac{\partial M}{\partial r}(r=R_p,t) = k_1\left(M_b - M\right) \tag{1c}$$

$$M(r,t=0) = M_0 = 0 \tag{1d}$$

where, R_{pv} is the rate of reaction per unit volume in

the macroparticle, D_{ef} is the effective diffusivity of monomer in the macroparticle, k_1 is the mass transfer coefficient in the external film, and M_b is the bulk monomer concentration in the reactor. M and M_0 are the evolving and the initial monomer concentrations in the macroparticle, respectively. R_p is the radial position at the macroparticle level of catalyst in this model as shown in Fig.1; since the catalyst fragments are assumed to be in a continuum of polymer also employed by Sarkar and Gupta[11] in PMGM, there is no macroparticle porosity term in Eq.(1) in contrast to that in MGM[9].

The radial profile of monomer concentration in the microparticle is the same as that for the SCM[6,7]:

$$\frac{\partial M_c}{\partial t}=\frac{1}{r^2}\frac{\partial}{\partial r}\left(D_s r^2\frac{\partial M_c}{\partial r}\right) \tag{2a}$$

$$4\pi R_c^2 D_s\frac{\partial M_c}{\partial r}\left(r=R_c,t\right)=\frac{4}{3}\pi R_c^3 R_{pc} \tag{2b}$$

$$M_c\left(r=R_s,t\right)=M^*=\eta^* M\leqslant M \tag{2c}$$

$$M_c\left(r,t=0\right)=M_{c0} \tag{2d}$$

where, D_s is the effective diffusivity of monomer in the microparticle, M^* is the equilibrium concentration of monomer in the interface between micro- and macroparticles, M_c is the monomer concentration in the microparticle, R_{pc} is the rate of polymerization on the surface of the catalyst fragments, and R_s is the radius of the microparticle. The boundary condition Eq.(2b) allows for the possibility of sorption equilibrium at the surface of the microparticles.

The rate of polymerization on the microparticles is generally given by:

$$R_{pc}=k_p(t)C^*(t)M_{SA} \tag{3}$$

where, M_{SA} is the concentration of monomer on the active site, and $C^*(t)$ is the time-dependent concentration of active sites on the surface of the microparticle.

Using the quasi steady state approximation (QSSA) presented by Hutchinson[10], M_c is easily obtained as:

$$M_c=\frac{\eta^* M}{1+\frac{R_c^2}{3D_s}\left(1-\frac{R_c}{R_s}\right)k_p C^*} \tag{4}$$

where M_c is the monomer concentration at the catalyst surface in the microparticle, and η^* represents the corresponding equilibrium constant for monomer absorption in the microparticle. Special attention must be payed to this point that the microparticle diffusion (D_s) through the polymer film surrounding the catalyst fragments is considered here as shown in Eq.(4), which is ignored by PMGM, and this is one of the contributions of this study.

The number of small particles in any shell, $N_{n,i}$, is assumed to be unchanged during the polymerization processes and all catalyst subparticle radii for each microparticle in the ith shell at a given macroparticle radius are all assumed to be of the same size[9]. Eq.(1) is then rewritten in finite difference form to provide a set of ordinary differential equations (ODEs) for M_i, the monomer concentration at each of the N_c+2 different computational grid points as shown in Fig.2, and the ODEs are listed as follows:

$$\frac{\partial M_1}{\partial t}=D_{ef,1}\frac{M_2-M_1}{\Delta r_1^2}-R_{pv,1} \tag{5a}$$

$$\begin{aligned}\frac{\partial M_i}{\partial t}=D_{ef,i}\Bigg[&M_{i+1}\left(\frac{1}{\Delta r_{c,i}R_{cg,i}}+\frac{1}{\Delta r_{c,i}^2}\right)-\\&M_i\left(\frac{1}{\Delta r_{c,i}^2}+\frac{1}{\Delta r_{c,i-1}\Delta r_{c,i}}\right)+\\&M_{i-1}\left(\frac{1}{\Delta r_{c,i-1}\Delta r_{c,i}}-\frac{1}{\Delta r_{c,i}R_{c,i}}\right)\Bigg]-R_{pv,i}\\&i=2,3,\cdots,N_c+1\end{aligned} \tag{5b}$$

$$\begin{aligned}\frac{\partial M_{N_c+2}}{\partial t}=&-M_{N_c+2}\times\\&\left[\frac{k_l}{\Delta r_{c,N_c+1}}+\frac{D_{ef,N_c+2}}{\left(\Delta r_{c,N_c+1}\right)^2}+\frac{2k_l}{R_{cg,N_c+2}}\right]+\\&M_{N_c+1}\left[\frac{2D_{ef,N_c+2}}{\left(\Delta r_{c,N_c+1}\right)^2}\right]+\\&M_b\left(\frac{k_l}{\Delta r_{c,N_c+1}}+\frac{2k_l}{R_{cg,N_c+2}}\right)-R_{pv,N_c+2}\end{aligned} \tag{5c}$$

where, $R_{cg,i}$, $\Delta r_{c,i}$, $D_{ef,i}$, $R_{pv,i}$ can be computed through the hypothetical clubbed shell that was defined (as shown in Fig.2).

According to Fig.2, the number of subparticles in the ith shell at time $t=0$, $N_{n,i}$, is calculated using the porosity ε, which has been taken to be a constant, as in the early MGM[9] in the polymerization process, associated with close-packed sphere:

$$N_{n,1}=1 \tag{6a}$$

$$N_{n,i}=24(1-\varepsilon)(i-1)^2\quad i=2,3,\cdots,N_c \tag{6b}$$

To reduce the computational effort, the spherical shell is supposed to be clubbed together into a less number (N_c). The fewer spherical shells can be clubbed together in regions where the monomer concentration varies significantly with the radius of the macroparticle, and several shells can be put together where the variation of monomer concentration with location is not as server. Therefore, it can be expressed in the following forms by assuming that $N-6$ can be divided by N_c-3:

$$N_{nn}(i)=\sum_{j=1}^{a}N_n\left[a(i-1)+j\right],a=\frac{N-6}{N_c-3}$$
$$i=1,2,\cdots,N_c-3 \tag{7a}$$

$$N_{nn}\left(N_c\right)=N_n\left(N-5\right)+N_n\left(N-4\right) \tag{7b}$$

$$N_{\mathrm{nn}}\left(N_{\mathrm{c}}-1\right)=N_{\mathrm{n}}\left(N-3\right)+N_{\mathrm{n}}\left(N-2\right) \tag{7c}$$

$$N_{\mathrm{nn}}\left(N_{\mathrm{c}}\right)=N_{\mathrm{n}}\left(N-1\right)+N_{\mathrm{n}}\left(N\right) \tag{7d}$$

The total volume of polymer, V_i, and the volume of microparticle at the ith shell, $V_{\mathrm{s},i}$, all produced by catalyst particles are given by:

$$\frac{\mathrm{d}V_i}{\mathrm{d}t}=0.001k_{\mathrm{p}}C^{*}M_{\mathrm{c},i}\left(N_{\mathrm{nn},i}\frac{4\pi}{3}R_{\mathrm{c}}^{3}\right)M_{\mathrm{W}}/\rho_{\mathrm{p}} \tag{8}$$

$$\frac{\mathrm{d}V_{\mathrm{S},i}}{\mathrm{d}t}=0.001k_{\mathrm{p}}C^{*}M_{\mathrm{c},i}\left(\frac{4\pi}{3}R_{\mathrm{c}}^{3}\right)M_{\mathrm{W}}/\rho_{\mathrm{p}}$$

$$i=1,2,\cdots,N_{\mathrm{c}} \tag{9}$$

with $V_i(t=0)$ and $V_{\mathrm{S},i}(t=0)$ being the initial total volume and the volume of every polymer microparticle of ith volume, respectively.

$$V_i(t=0)=N_{\mathrm{nn},i}\left(\frac{4\pi}{3}R_{\mathrm{c}}^{3}\right)/(1-\varepsilon);\quad i=1,2,\cdots,N_{\mathrm{c}} \tag{10}$$

$$V_{\mathrm{S},i}\left(t=0\right)=\frac{4\pi}{3}R_{\mathrm{c}}^{3} \tag{11}$$

The $M_{\mathrm{c},i}$ is the modified monomer concentration value of the catalyst surface in the microparticle at the ith hypothesis clubbed shell, $R_{\mathrm{ch},i}$, computed by Eq.(4); the detailed form is expressed as follows:

$$M_{\mathrm{c},i}=\frac{\eta M_{i+1}}{1+\dfrac{R_{\mathrm{c}}^{2}}{3D_{\mathrm{s}}}\left(1-\dfrac{R_{\mathrm{c}}}{R_{\mathrm{s},i}}\right)k_{\mathrm{p}}C^{*}} \tag{12}$$

This point is amended to perfect PMGM by taking the factor of diffusion at the microparticle level under advisement. The detailed form of Eq.(4) originates from this reason.

The hypothesis clubbed shells at any time, $R_{\mathrm{ch},i}$, can be defined by:

$$R_{\mathrm{ch},i}=\left(\frac{3}{4\pi}\sum_{j=1}^{i}V_j\right)^{1/3},\qquad i=1,2,\cdots,N_{\mathrm{c}} \tag{13}$$

where, $R_{\mathrm{ch},0}=0$, and the radius of the microparticle at the ith clubbed shell is:

$$R_{\mathrm{s},i}=\left(\frac{3}{4\pi}V_{\mathrm{s},i}\right)^{1/3} \tag{14}$$

The finite difference grid points in the clubbed shell algorithm can now be assumed to be placed at the mid points of the hypothetical clubbed shells (see Fig.2). The grid point locations are thus given by:

$$R_{\mathrm{cg},1}=0 \tag{15a}$$

$$R_{\mathrm{cg},2}=\frac{R_{\mathrm{h},1}}{2} \tag{15b}$$

$$R_{\mathrm{cg},i+1}=R_{\mathrm{h},i-1}+\frac{R_{\mathrm{h},i}-R_{\mathrm{h},i-1}}{2}\qquad i=2,3,\cdots,N_{\mathrm{c}} \tag{15c}$$

$$R_{\mathrm{cg},N_{\mathrm{c}}+2}=R_{\mathrm{h},N_{\mathrm{c}}} \tag{15d}$$

The value of the distances between the grid points, which are used in Eqs.(5), are given by:

$$\Delta r_{\mathrm{c},1}=\frac{R_{\mathrm{h},1}}{2} \tag{16a}$$

$$\Delta r_{\mathrm{c},i}=R_{\mathrm{cg},i+1}-R_{\mathrm{cg},i}\qquad i=2,3,\cdots,N_{\mathrm{c}}+1 \tag{16b}$$

To account for the resistance due to the presence of the solid catalyst fragments after completing all

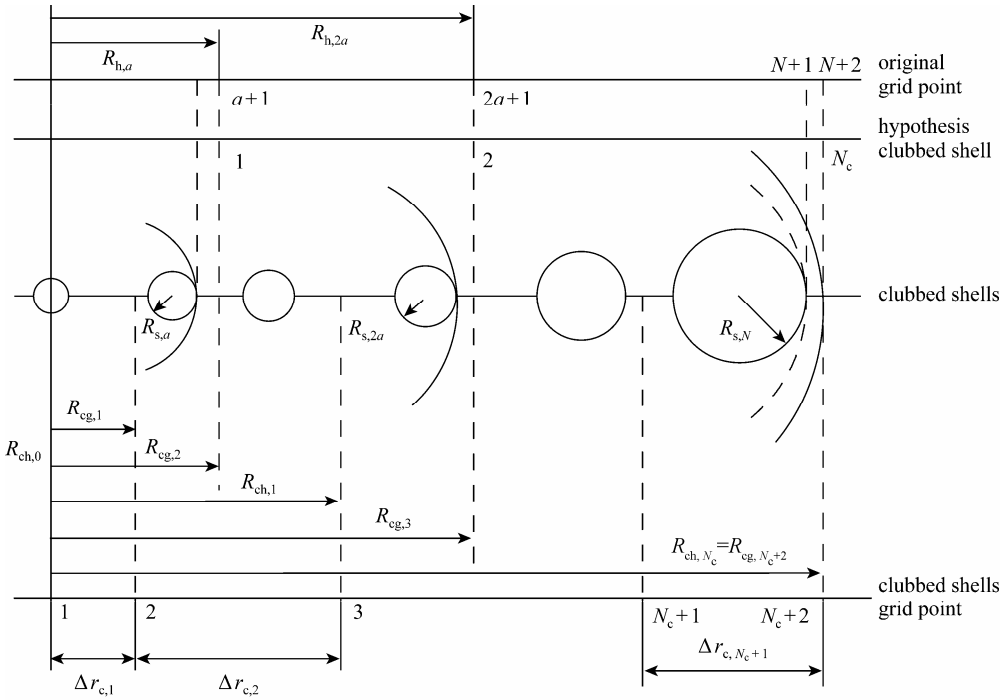

Figure 2 Catalyst subparticles distribution in the modified polymeric multigrain model with clubbing

[Where a is calculated by Eq.(7a)]

previous work, an effective diffusivity is introduced into this equation. Most models have tried to relate the effective diffusivity, D_{ef}, to the value of the diffusivity of the component in the bulk phase of the reactor, D_l, using the following expression commonly used for heterogeneous catalysts:

$$D_{ef} = D_l \cdot \frac{\varepsilon}{\tau} \tag{17}$$

where, ε and τ are the porosity and tortuosity of the macroparticle, respectively. Note that owing to the macro-particle fragmentation and growth, it is very likely that both ε and τ are functions of time as well as the radial position. Sarkar and Gupta[11,12] corrected the diffusivity by a factor proportional to the amount of polymer in the particles, *i.e.* the term ε/τ of the above-mentioned equation, for a correction factor equal to the area-fraction of polymer (assumed to be the same as its volume fraction) in the macroparticle at any radial location. Thus, as the particle fills up with polymer, the effective diffusivity decreases as follows:

$$D_{ef,1} = D_{ef,N_c+2} = D_l \tag{18a}$$

$$D_{ef,2} = D_l N_{nn,1} \frac{R_c^3}{R_{h,1}^3} \tag{18b}$$

$$\begin{aligned} D_{ef,i+1} &= D_l \frac{\left(V_{cs,i} - V_{cc,i}\right)}{V_{cs,i}} \\ &= D_l \frac{R_{h,i}^3 - R_{h,i-1}^3 - N_{nn,i} R_c^3}{R_{h,i}^3 - R_{h,i-1}^3} \end{aligned} \tag{18c}$$

where, D_l is the diffusion of the monomer through pure polymer, and $V_{cs,i}$ and $V_{cc,i}$ are the volume of the ith hypothesis shell and the volume of the catalyst in shell i, respectively. Thus, the effective diffusion coefficient considered here is changed at any time during particle growth in opposition to Floyd *et al.*[9].

The net rates of consumption of monomer per unit macroscopic volume at any radial location at the mean time are then figured out by:

$$R_{pv,1} = R_{pv,N_c+2} = 0 \tag{19a}$$

$$R_{pv,2} = \frac{k_p C^* M_{c,1} N_{nn,1} R_c^3}{R_{h,1}^3} \tag{19b}$$

$$R_{pv,i} = \frac{k_p C^* M_{c,i-1} N_{nn,i-1} R_c^3}{R_{h,i}^3 - R_{h,i-1}^3} \tag{19c}$$

Therefore, the corresponding overall time-dependent particle polymerization rate, which is closely related to the reactor stability and safety, is given by:

$$R_o = \frac{0.001 M_W k_p C^* \sum_{i=1}^{N_c} \left(N_{nn,i} M_{c,i}\right)}{\rho_c \sum_{i=1}^{N_c} N_{nn,i}} \tag{20}$$

2.2 Extended convection-diffusion model

It may be universally acknowledged that most values obtained by pure Fick's diffusion model at the mesoscale level agree reasonably well with the experimental measurements[18] for both microparticles and macroparticles. It is, however, important to point out that the diffusion coefficients may not be directly applicable to the dynamic and rather complex processes occurring during the growth of polyolefin particles.

McKenna and Soares[19] first advances that under certain circumstance, mass transport in the growing particles is not only by Fician diffusion alone, but also by convection, which is driven by the pressure gradient created by the monomer consumption within the particle. According to the significant number of open literature on this part, the convection and diffusion can be modeled by two different ways, advection-dispersion model (ADM) and dusty gas model (DGM)[20,21]. In this article, the ADM model, based on simple linear addition of diffusion and convection[22], is mainly presented to confirm the efficiency of this calculational method using the clubbed shells algorithm mentioned above. The detailed model is presented as follows.

It is considered that the growing polymer particle is also made up of spherical particles. Eq.(21) is used to describe the mass transport caused by both convection and diffusion with no inert gases, because gas phase propylene polymerization is done in the presence of a significant amount of inert gases for the most part, in which case, the convective mass transfer will probably be negligible.

$$\begin{aligned} \frac{1}{R_g T}\frac{\partial\left(x_1 P\right)}{\partial t} = \frac{1}{r^2}\frac{\partial}{\partial r}\Bigg[r^2 \frac{D_{ef}}{R_g T}\frac{\partial\left(x_1 P\right)}{\partial r} + \\ \frac{1}{R_g T}\frac{1}{\mu_g} B_0 r^2 \left(x_1 P\right)\frac{\partial p}{\partial r}\Bigg] - R_v \end{aligned} \tag{21}$$

where, $B_0 = \frac{2\varepsilon}{9\tau(1-\varepsilon)} R_s^2$ is the viscous flow parameter dependent on the porosity (ε) and tortuosity (τ); P is monomer pressure, Pa; μ_g is monomer viscosity, Pa·s; R_v is the rate of reaction based on polymer volume, mol·m^{-3}·s^{-1}. The pore radius is considered to be the same as the radius of the final microparticle.

When considering gas phase polymerization, it can be assumed that the gaseous monomer in the pores of the macroparticle behaves as an ideal gas with concentration $M = P/R_g T$; Eq.(21) is then finally rewritten as:

$$\frac{\partial M}{\partial t} = \frac{1}{r^2}\frac{\partial}{\partial r}\left[r^2 \left(D_{ef} + \frac{R_g T}{\mu_g} B_0 M \right)\frac{\partial M}{\partial r}\right] - R_v \tag{22}$$

Using our previous solution method, the clubbed shells algorithm, which has been proved to be able to improve the computational rate significantly, Eq.(22) is changed to the following form:

$$\frac{\partial M_i}{\partial t} = D_{\mathrm{ef},i}\left[M_{i+1}\left(\frac{1}{\Delta r_{\mathrm{c},i}R_{\mathrm{cg},i}}+\frac{1}{\Delta r_{\mathrm{c},i}^2}\right)-M_i\left(\frac{1}{\Delta r_{\mathrm{c},i}^2}+\frac{1}{\Delta r_{\mathrm{c},i-1}\Delta r_{\mathrm{c},i}}\right)+M_{i-1}\left(\frac{1}{\Delta r_{\mathrm{c},i-1}\Delta r_{\mathrm{c},i}}-\frac{1}{\Delta r_{\mathrm{c},i}R_{\mathrm{cg},i}}\right)\right]+\beta_{\mathrm{i}}\left[M_{i+1}^2\left(\frac{1}{\Delta r_{\mathrm{c},i}R_{\mathrm{cg},i}}+\frac{1}{\Delta r_{\mathrm{c},i}^2}\right)-M_i^2\left(\frac{1}{\Delta r_{\mathrm{c},i}^2}+\frac{1}{\Delta r_{\mathrm{c},i-1}\Delta r_{\mathrm{c},i}}\right)+M_{i-1}^2\left(\frac{1}{\Delta r_{\mathrm{c},i-1}\Delta r_{\mathrm{c},i}}-\frac{1}{\Delta r_{\mathrm{c},i}R_{\mathrm{cg},i}}\right)\right]-R_{\mathrm{v},i} \tag{23}$$

where, $\beta_{\mathrm{i}} = \frac{R_{\mathrm{g}}T}{\mu_{\mathrm{g}}}\frac{\varepsilon}{9\tau(1-\varepsilon)}R_{\mathrm{s},i}^2$ is an indicator of the monomer convection contribution in contrast with the diffusion. Then, the corresponding overall time-dependent reaction rate ($\mathrm{g\cdot g^{-1}\cdot h^{-1}}$, based on catalyst) is calculated as follows:

$$R_{\mathrm{o}} = \frac{0.001M_{\mathrm{W}}k_{\mathrm{p}}C^*\sum_{i=1}^{N_{\mathrm{c}}}\left(N_{\mathrm{nn},i}M_{\mathrm{c},i}\right)}{\rho_{\mathrm{c}}\sum_{i=1}^{N}N_{\mathrm{c},i}} \tag{24}$$

where, M_{W} is the molecular weight of the propylene monomer and k_{p} is the propagation rate constant ($\mathrm{m^3\cdot mol^{-1}\cdot s^{-1}}$). In the absence of diffusion limitations, its maximum possible value is obtained from the catalyst's intrinsic reactivity by:

$$R_{\max} = R_{\mathrm{in}} = \frac{k_{\mathrm{p}}C^*M_{\mathrm{b}}M_{\mathrm{W}}}{\rho_{\mathrm{c}}} \tag{25}$$

3 RESULTS AND DISCUSSION

The simulation of this ODEs system on calculating the value of monomer concentration is solved using the Runge-Kutta-Fehlberg method[23]. This section is divided into three subsections for better discussion. The former two subsections explain several developments of this modified PMGM model in comparison with the original PMGM model[11,12] on PDI, monomer concentration, and average degree of polymerization when changing some key relevant parameters. The overall polymerization rate and computational time are analyzed between the pure Fickian diffusion model and the convection-diffusion model in the last subsection.

3.1 Comparison on PDI and monomer concentration

Figure 3 shows the comparison of the cumulative polydispersity index (Q_{av}) and the distribution of monomer concentration in the macroparticle between modified PMGM and PMGM for the reference conditions in Table 2 also employed by Sarkar and Gupta[12]. In theory, the diffusion resistance abandoned by PMGM obviously exists and must be put up in the mesoscale model. The modified PMGM, however, revises it and can predict higher values of polydispersity index from 6 to 25 when compared to that of PMGM (from 4 to 15) as shown in Fig.3(a) owing to the steeper modified monomer concentration profile as

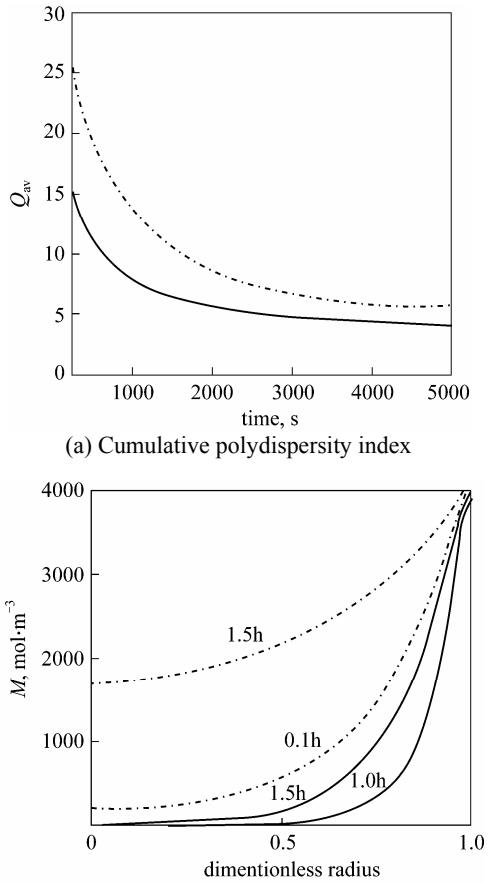

(a) Cumulative polydispersity index

(b) Monomer concentration

Figure 3 Comparison of the cumulative polydispersity index and monomer concentration
—— PMGM; - - - - modified PMGM

Table 2 Reference values of parameters for simulation of slurry polymerization of propylene

D_l, $\mathrm{m^2\cdot s^{-1}}$	D_{s}, $\mathrm{m^2\cdot s^{-1}}$	M_{b}, $\mathrm{mol\cdot m^{-3}}$	R_{c}, m	C^{*}①	k_{p}, $\mathrm{m^3\cdot mol^{-1}}$	k_{tr}, $\mathrm{m^{3/2}\cdot mol^{-1/2}\cdot s^{-1}}$	H_2, $\mathrm{mol\cdot m^{-3}}$	ρ_{p}, $\mathrm{kg\cdot m^{-3}}$	ρ_{c}, $\mathrm{kg\cdot m^{-3}}$
1×10^{-10}	1×10^{-12}	4×10^{3}	2×10^{-7}	1	0.5	0.186	1	900	2260

① The unit of C^* is active site based on $1\mathrm{m^3}$ catalyst.

shown in Fig.3(b) in the catalyst macroparticles, which is more reasonable while talking in physics meaning.

The monomer concentration at the macroparticle level of PMGM as shown in Fig.3(b) is not applicable to the conditions existing in most polymerization of industrial interest since the monomer concentration at the center of the particles drops very quickly to nearly zero and remains there for over 2h of polymerization[3]. The proposed model modified it, which is displayed in Fig.3(b) with the dash-dot line, and the monomer concentration at the center of the particle is about 1800mol·m^{-3} after 1.5h polymerization reaction, which is closer to the industrial practice.

3.2 Effect of the radius of the microparticle

The results for the modified PMGM are generated under the conditions of changing the radius of microparticle (R_c) while keeping the initial particle radius (R_0) as constant. The detailed descriptions of the material balance, the moment equation, the computational method of PDI, and the measurement of MWD are well documented by open literatures in this area[9,24].

Nagel *et al*.[6] notes that the constant number of subparticles induced by the instantaneous rupture of catalyst macroparticle has a strong influence on the polydispersity. PMGM indicates, however, that there is not much change to the results under such circumstance. This result does not correspond to the actual physical process obviously. It is revised by this modified PMGM, and it can be observed from Fig.4 that Q_{av} of the polymer decreases while D_{Pav} increases when R_0 is lowered from 14.2 to 7.1μm in the condition that all other values are constant. The reason why D_{Pav} is higher for lower values of R_0 is that the lower diffusional resistances encountered in smaller catalyst particles will make the difference of monomer concentration between the inside and outside of the particle diminish. It is also found that D_{Pav} is very sensitive to the parameter of R_c while retaining C^* constant, namely, C^* has no connection with the total surface area of the microparticle. Similarly, as seen in Fig.4, D_{Pav} and Q_{av} go in an opposite direction; the former increases while the latter decreases while varying R_c from 0.3 to 0.1μm at the same value of R_0. Thus, with single site catalysts, both larger initial catalyst particles and larger subparticles can give rise to high PDIs.

3.3 Analysis for the reaction rate and the computational time

Another interesting aspect of this investigation is the efficiency of the extended clubbed shells algorithm, which enables a simpler mathematical representation. It is, moreover, important to point out that the improved algorithm can easily be extended to model industrial problems where additional physicochemical effects are present, such as the studies of more practical convection-diffusion model in the last decade to explain some phenomena, which the pure Fickian's diffusion model fails to reach under certain circumstance[3]. The comparison of the overall polymerization rate, which is closely related to the reactor stability and safety, between the Fickian model and the convective model is shown in Table 3.

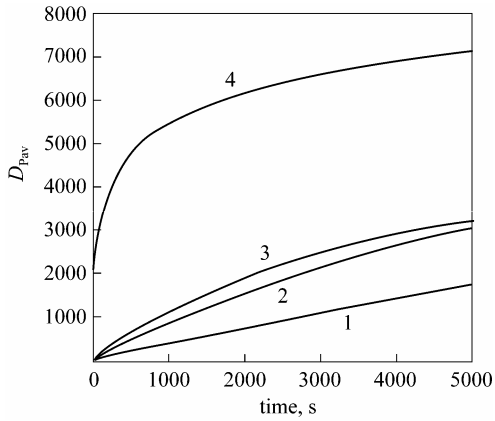

(a) On the degree of polymerization

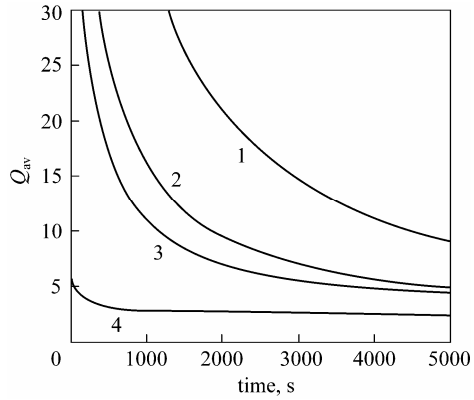

(b) On the cumulative polydispersity index

Figure 4 Effect of the change in R_c while maintaining R_0 unchanged

1—R_c=0.3μm, R_0=14.2μm; 2—R_c=0.2μm, R_0=14.2μm; 3—R_c=0.1μm, R_0=14.2μm; 4—R_c=0.1μm, R_0=7.1μm

Table 3 Comparison of the peak overall polymerization rate between Fickian diffusion and convective model①

R_{in}, g·g^{-1}·h^{-1}	R_o of Fickian diffusion model, g·g^{-1}·h^{-1}	R_o of convective model, g·g^{-1}·h^{-1}
4.0×10^4	$25\times10^3(29\times10^3)$	$37\times10^3(38\times10^3)$
1×10^5	$50\times10^3(53\times10^3)$	$95\times10^3(96\times10^3)$

① Values in brackets are obtained by Veera[21].

Table 3 reveals that the Fickian diffusion model predicts low reactivity when compared to the convection-diffusion model for its high diffusional limitations, and fails to interpret the high reaction rate now attainable, which is explicitly noted by McKenna and Soares[3]. Thus, all these peak values of reaction rates, 25kgPP/60g catalyst per hour for the Fickian diffusion model, and 37kgPP/95g catalyst per hour for the Convective-diffusion model calculated from transport models with clubbed shells algorithm while adopting the typical parameter values suggested by Veera[20], are in substantial agreement with those discussed in

Table 4 Computational time (Pentium IV 1.7G/256M) for the reference run

Shell by shell algorithm			Clubbed shells algorithm		
PMGM	Modified PMGM	Convection diffusion model	PMGM	Modified PMGM	Convection-diffusion model
28s	38s	110s	2s	4s	7s

Veera's literature[21] on gas phase propylene polymerization, 29kgPP/53g catalyst per hour for the Fickian diffusion model and 38kgPP/96g catalyst per hour for the convective-diffusion model. Other relative detailed discussions and analysis about the convective model are in progress since it is very important and is worth deep research.

Another main purpose of this subsection is to compare the computational time among the original PMGM model, the modified PMGM model, and the convection-diffusion model besides ensuring that the outcome is reasonable. The CPU time for solving these three models with the two different algorithms is listed in Table 4, where the CPU time of the three models with shell by shell algorithm and clubbed shell algorithm are reduced from 28s, 38s, 110s to 2s, 4s, 7s, respectively. It reveals the visible advantages of the clubbed shells algorithm, which implements very easily and accelerates the computation time significantly in contrast to the normal shell by shell algorithm, which is used by most researchers[6,7,11] to solve the mass transfer model.

4 CONCLUSIONS

The modified PMGM model has been advanced to amend some unreasonable conclusions of the PMGM model since the monomer concentration at the centre of the particles drops very quickly to nearly zero and remains there for over 2h of polymerization, while changing R_c does not lead to considerable change in the results with the single site catalyst. It has been found from this model, however, that D_{Pav} and PDI are very sensitive to the parameter of R_c when it has no connection with the total surface area of the microparticle. It is also shown that D_{Pav} and Q_{av} go in opposite directions; the former increases whereas the latter decreases while reducing R_c and maintaining R_0 as constant.

Additionally, the idea of the clubbed shells algorithm has been successfully applied to solve the dynamic equations with the expansion model of both the Fickian diffusion model and the convection-diffusion model. The improvement of this method is that it requires far fewer discretizations in the space domain than normal finite differences and thus shortens the computational time significantly. Furthermore, it can easily be extended to work for more complex and practical industrial phenomenon and application while maintaining reasonable results simultaneously on mesoscale phenomena as shown in the present study, where the predictive values of some important parameters, such as the cumulative polydispersity index, are necessary for further macroscale reactor modeling researches of propylene polymerization.

NOMENCLATURE

C^*	catalyst active site concentration, mol site·m^{-3}
$D_{ef,i}$	effective macroparticle diffusion coefficient, at ith grid point, m^2·s^{-1}
D_l	monomer diffusivity in pure polymer, m^2·s^{-1}
D_{Pav}	degree of polymerization in the macroparticle
D_s	effective microparticle diffusion coefficient
k_l	liquid film mass transfer coefficient, m^2·s^{-1}
k_p	propagation rate constant, m^3 ·mol^{-1}·s^{-1}
k_{tr}	chain transfer rate constant, for H_2, m$^{3/2}$· mol$^{1/2}$·s^{-1}
M_b	bulk monomer concentration, mol·m^{-3}
$M_{c,i}$	modified monomer concentration at the catalyst surface in the microparticle, at the ith shell, mol·m^{-3}
M_i	monomer concentration in the macroparticles, at the ith grid point, mol·m^{-3}
M_W	molecular weight of monomer, g·mol^{-1}
N	number of EA shells
N_c	number of clubbed shells
$N_{n,i}$	number of catalyst subparticles in the ith hypothesis shell monomer units attached (based on catalyst), mol·m^{-3}
$N_{nn,i}$	number of catalyst subparticle in ith clubbed monomer units attached (based on catalyst), mol·m^{-3}
Q_{av}	cumulative polydispersity index
R_0	initial particle radius of catalyst macroparticle at $t=0$, m
R_c	radius of catalyst microparticle or fragment, m
$R_{cg,i}$	radius at the ith clubbed shell grid point
$R_{ch,i}$	radius of the ith hypothetical clubbed shell
R_g	universal gas constant, Pa·m^3·mol^{-1}·K^{-1}
$R_{h,i}$	radius of the ith hypothetical shell at original grid point
R_{N+2}	macroparticle radius, m
R_o	time-dependent reaction rate per kg catalyst, kg·s^{-1}
R_p	radial position at the macroparticle level of catalyst, m
R_{pv}	rate of reaction per unit volume in the macroparticle, mol·m^{-3}s^{-1}
$R_{pv,i}$	rate of reaction per unit volume in the macroparticle at the ith grid point, mol·m^{-3}s^{-1}
$R_{s,i}$	radius of microparticle at the ith shell
R_v	rate of reaction based on polymer volume, mol·m^{-3}s^{-1}
$\Delta r_{c,i}$	value of distances between the ith and (i+1)th clubbed shell grid point, m
T	temperature, K
t	time, h
β_i	indicator of the monomer convection contribution
ε	porosity
η	monomer sorption coefficient
μ_g	monomer viscosity, Pa·s
ρ_c	density of catalyst, g·m^{-3}
ρ_p	density of polymer, g·m^{-3}
τ	tortuosity

REFERENCES

1 Moore, J.E.P., Larson, G.A., "Introduction to PP in business", Polypropylene handbook, Hanser Publishers, Cincinatti (1996).

2 Shi, J., Liu, X.G., "Melt index prediction by neural soft-sensor based on multi-scale analysis and principal component analysis", *Chin. J. Chem. Eng.*, **13**(6), 849—852(2005).

3 McKenna, T.F., Soares, J.B.P., "Single particle modeling for olefin polymerization on supported catalysts: A review and proposals for future developments", *Chem. Eng. Sci.*, **56**(13), 3931—3949(2001).

4 Fan, S.J., Xu, Y.M., "Modeling of propylene polymerization: Effect of diffusion", *J. Ch. Ind. Eng.*, **51**(6), 771—776(2000). (in Chinese)

5 Gao, Y., Chen, D.Z., Hua, W.Q., Hu, S.X., "Development of full flow-sheet operator training simulator for spheripol PP monopolymerization plant", *Comput. Simul.*, **15**(4), 17—20(1998). (in Chinese)

6 Nagel, E.J., Krillov, V.A., Ray, W.H., "Prediction of molecular weight distributions for high density polyolefins", *Ind. Eng. Chem. Prod. Res. Dev.*, **19**, 372—379(1980).

7 Schmeal, W.R., Street, J.R., "Polymerization in expanding catalyst particles", *AIChE J.*, **17**(5), 1188—1197(1971).

8 Yiagopoulos, A., Yiannoulakis, H., Dimos, V., Kiparissides, C., "Heat and mass transfer phenomena during the early growth of a catalyst particle in gas-phase olefin polymerization: The effect of prepolymerization temperature and time", *Chem. Eng. Sci.*, **56**, 3979—3995(2001).

9 Floyd, S., Herskanen, T., Taylor, T.W., Mann, G.E., Ray, W.H., "Polymerization olefins through heterogeneous catalysts (Ⅵ) Effect of particle heat and mass transfer on polymerization behavior and polymer particles", *J. Appl. Polym. Sci.*, **33**, 1021—1065(1987).

10 Hutchinson, R.A., Chen, C.M., Ray, W.H., "Polymerization of olefins through heterogeneous catalysts (Ⅹ) Modelling of particle growth and morphology", *J. Appl. Polym. Sci.*, **44**, 1389—1414(1992).

11 Sarkar, P., Gupta, S.K., "Modelling of propylene polymerization in an isothermal slurry reactor", *Polymer*, **32**(5), 2842—2852(1991).

12 Sarkar, P., Gupta, S.K., "Simulation of propylene polymerization: An efficient algorithm", *Polymer*, **33**, 1477—1485(1992).

13 Laurence, R.L., Chiovetta, M.G., "Heat and mass transfer during olefin polymerization from the gas phase", In: Polym. React. Eng., Reichert, K.H., Geiseler, W., eds., Hanser Verlag, Munich, 71—112(1983).

14 Kittilsen, P., Svendsen, H., McKenna, T.F., "Modeling of transfer phenomena on heterogeneous Ziegler catalyst (Ⅳ) Convection effects in gas phase processes", *Chem. Eng. Sci.*, **56**, 3997—4005(2001).

15 Kakugo, M., Sadatoshi, H., Sakai, J., Yokoyama, M., "Growth of polypropylene particles in heterogeneous Ziegler-Natta polymerization", *Macromolecules*, **22**(7), 3172—3177(1989).

16 Estenoz, D.A., Chiovetta, M.G., "Olefin polymerization using supported metallocene catalysts: Process representation scheme and mathematical model", *J. Appl. Polym. Sci.*, **81**(2), 285—311(2001).

17 Ferrero, M.A., Chiovetta, M.G., "Catalyst fragmentation during propylene polymerization (Ⅰ) The effects of grain size and structure", *Poly. Eng. Sci.*, **27**(19), 1436—1447(1987).

18 Sliepcevich, A., Storti, G., Morbidelli, M., "Measurement of diffusivity and solubility of olefins in polypropylene by gas chromatography", *J. Appl. Polym. Sci.*, **78**(2), 464—473(2000).

19 McKenna, T.F., Soares, J.B.P., "Modelling of transport phenomena on heterogeneous Ziegler catalysts: Modeling of intraparticle mass transfer resistance", *J. Appl. Polym. Sci.*, **63**, 315—322(1997).

20 Veera, U.P., Weickert, G., "Modeling monomer transport by convection during olefin polymerization", *AIChE J.*, **48**(5), 1062—1070(2002).

21 Veera, U.P., "Mass transport models for a single particle in gas-phase propylene polymerization", *Chem. Eng. Sci.*, **58**(9), 1765—1775(2003).

22 Veldsink, J.W., Damme, R.M.J., Versteeg, G.F., Swaaij, W.P.M., "The use of dusty gas model for the description of mass transport with chemical reaction in porous media", *Chem. Eng. J.*, **57**(2), 115—125(1995).

23 Fehlberg, E., "Some old and new Runge-Kutta formulas with stepsize control and their error coefficients", *Computing*, **34**(3), 265—270(1985).

24 Galvan, R., Tirrell, M., "Orthogonal collocation applied to analysis of heterogeneous Ziegler-Natta polymerization", *Comput. Chem. Eng.*, **10**(1), 77—86(1986).